The evolution of a gypsum vein network in compressive tectonic settings: the Montsant anticlinorium case (NE Spain)

La evolución de una red de venas de yeso en contextos tectónicos compresivos: El caso del anticlinorio del Montsant (NE España)

Cristina Martínez Rodríguez[1], Elisabet Playà Pous[1], Albert Griera Artigas[2] and Enrique Gómez Rivas[3]

[1] Departament de Geoquímica, Petrologia i Prospecció Geològica, Facultat de Geologia, Universitat de Barcelona, Martí i Franquès s/n, 08028, Barcelona, Spain. tina@vallat.net, eplaya@ub.edu

[2] Departament de Geologia, Universitat Autònoma de Barcelona, 08193, Cerdanyola del V., Spain. albert.griera@gmail.com

[3] Department of Geology and Petroleum Geology, University of Aberdeen, Aberdeen AB24 3UE, UK. e.gomez-rivas@abdn.ac.uk

ABSTRACT

The Montsant anticlinorium is part of the Pàndols-Cavalls-Montsant tectonic line situated in the southwestern area of the Catalan Coastal Ranges, adjacent to the contact with the Tertiary Ebro Basin. We have interpreted this Alpine structure as a triangular type I zone with two opposite faults. The centre of the anticlinorium is formed by middle Muschelkalk facies with intensively deformed gypsum layers and an intensively deformed zone with an associated framework of satin spar gypsum veins. A field structural analysis reveals that there are two sets of veins: one associated with a pre-folding stage (before the Alpine orogeny), and another one related to the development of the Montsant anticlinorium, and therefore syn-folding (and Alpine in age).

Key-words: *gypsum rocks, gypsum veins, Middle Muschelkalk, Alpine orogeny, structural analysis.*

RESUMEN

El anticlinorio del Montsant forma parte de la línea tectónica de Pándols-Cavalls-Montsant, situada al Suroeste de la Cordillera Costera Catalana, y adyacente al contacto con la Cuenca del Ebro. Esta estructura Alpina se interpreta como una zona triangular de Tipo I con dos flancos opuestos. El centro del anticlinorio está formado por facies del Muschelkalk medio con capas de yeso altamente deformadas formando una red de venas de yeso de tipo satin spar. *Mediante un análisis estructural de campo hemos identificado dos conjuntos de venas: uno asociado a la etapa previa al plegamiento (antes de la orogenia Alpina) y el otro asociado a la formación del anticlionorio del Montsant durante la orogenia Alpina.*

Palabras clave: *rocas de yeso, venas de yeso, Muschelkalk medio, orogenia Alpina, análisis estructural.*

Geogaceta, 60 (2016), 15-18
ISSN (versión impresa): 0213-683X
ISSN (Internet): 2173-6545

Recepción: 1 de febrero de 2016
Revisión: 20 de abril de 2016
Aceptación: 20 de Mayo de 2016

Introduction

Most of the literature dealing with gypsum precipitates in fractures focuses on fibrous gypsum veins (*satin spar*), and proposes that fibrous fillings are cements formed in open fracture planes (El Tabakh *et al*., 1998; Moragas *et al*., 2013; among others). Generally, satin spar veins are observed in relatively undeformed evaporite units and sub-parallel to bedding. However, complex polygenetic gypsum vein networks are commonly observed in thrust belts when detachment levels are localized within evaporites. This contribution presents a structural analysis of a series of deformed gypsum layers and veins cropping out at the core of the Montsant anticlinorium. Our main objective is to understand the relationship between the vein network and the local deformation during the Alpine orogeny.

Geological setting

The study area is located in the southwestern of the Catalan Coastal Ranges (CCR), close to its NW contact with the Tertiary Ebro Basin (Fig. 1A). The main structures of the CCR are NE-SW-trending polygenic basement faults, which acted as normal faults during the Mesozoic. Later on, they were reactivated as sinistral-reverse faults that produced the inversion of the Mesozoic rifted basins during the compressive Alpine orogeny (*e.g.*, Guimerà, 1984). These basement faults controlled the deposition of the Tertiary cover and produced the development of a narrow band of intensive deformation (the Pàndols-Cavalls-Montsant tectonic line, PCM in Fig. 1B; Teixell, 1988) between two relative undeformed areas (the Ebro and Mora basins) (Fig. 1B). This tectonic line consists of a NE-SW elongate anticlinorium (Fig. 1). Fission track data indicate uplift and exhumation of the area during the Upper Cretaceous (Juez-Larré and Andriessen, 2006), and coherent with Cornudella group that predate main Alpine phase (Teixell, 1998).

The study area is located at the centre of this anticlinorium, along the Montsant river transverse, between the villages of La Villella Baixa and Cabacès (Fig. 1B). In this

area, different units with ages ranging between the Paleozoic and Tertiary crop out. A series of folds and thrusts affect the sedimentary cover. This study focuses on Middle Muschelkalk (M2) evaporites.

Methods

A detailed structural analysis of gypsum vein sets was performed in order to identify whether each gypsum vein filled with fibrous cement formed pre- or syn-tectonically with folding and thrusting. For this purpose, data were collected at three different localities: one at the middle of the high-strain zone (outcrops B1 and B2; Fig. 2), and two located at the two limbs of the anticlinorium, which are low-deformed regions (outcrops A and C, at the western and eastern fold limbs, respectively; Fig. 2). The relative angle between the vein wall and fibres was measured in the field using a protractor. The extensional direction was obtained using the convic method of Durney and Ramsay (1973). This method assumes that the extensional direction lays at the acute bisector between the vein normal and the fibres. In the high-strain bands the analyses were restricted to a 2D section using the software FraNEP (Fracture Network Evaluation Program; Zeeb *et al.*, 2013). This code allows an automatic statistical analysis of 2D vein networks, and constructs rose diagrams of wall veins and gypsum fibre orientations.

Results and discussions

Middle Muschelkalk facies are composed of red siltstones interbedded with secondary gypsum layers, which comprise two different lithofacies (laminated-to-nodular gypsum and gypsum breccia). Secondary gypsum is formed by hydration of anhydrite. The M2 rocks host a dense network of veins that range from several dm to tens of meters in length and from less than 5 mm to more than 10 cm in width. These veins are parallel-to-oblique to the evaporite layers and are also hosted in the red siltstone interlayers.

Deformation appears strongly localized in a narrow synform band (high strain zone, Fig. 2) where intense folding of the M2 between the two thrusts with opposite vergence can be identified (*i.e.,* facing to the foreland and the hinterland). A main thrust facing towards the foreland is found at the SE flank of the anticlinorium. The map, cross section (Fig. 2, outcrops B1 and B2) and field observations indicate that this structure corresponds to a vertical thrust with an associated hanging-wall anticline and a steeply dipping back-limb on the SE. The thrust facing towards the hinterland is observed at the NW flank of the anticlinorium and dips subvertically. Based on the cross section (Fig. 2), values of displacement range between approx. 250 m for the foreland thrust and less than 100 m for the backthrust. The structure corresponds to a "pop-down" or a type I triangular zone according to Couzens and Wiltschko (1996). Both thrusts develop a damage zone formed by breccias and reddish-brown gouge. A dense and complex network of gypsum veins, as well as large pieces of brecciated and laminated gypsum, are observed at the core of this structure. The maximum vein density is found at the high strain zone in the hinge of the synform, while gypsum veins sharply disappear near the damage zone associated with both faults (Fig. 3H).

Infilling formed in the following sequence (in chronological order): *a)* fibrous gypsum (*satin spar*) cements growing perpendicular to vein walls, and, *b)* large prismatic (or subeuhedral) crystals that can partially or almost entirely overprint the fibrous crystals and grow from parallel to slightly oblique to the fibres. Although all described infillings can appear in all veins, veins hosted in the laminated-to-nodular and brecciated host unit (A

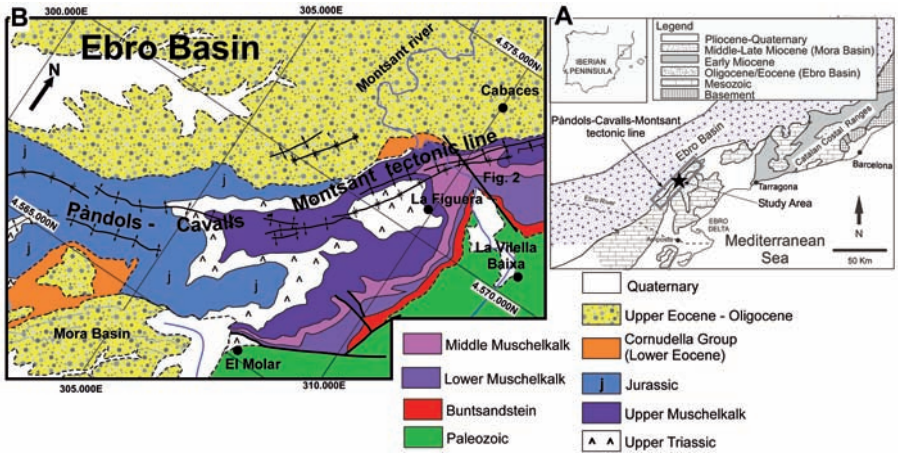

Fig. 1.- A) Simplified geological sketch of the Catalan Coastal Ranges in contact with the Ebro foreland basin. The Pàndols-Cavalls-Montsant tectonic line is indicated with a grey rectangle and the study area with a star. Modified from Playà et al. (2010). B) Geologic map of the studied área (modified from Institut Cartogràfic i Geologic de Catalunya, 2006). See colour figure on the Web.

Fig. 1- A) Esquema geológico simplificado de la Cordillera Costera Catalana en contacto con la cuenca del Ebro. La línea tectónica de Pàndols-Cavalls-Montasant está indicada con un rectángulo gris y la zona de estudio con una estrella negra. Modificado de Playà et al. (2010). B) Mapa geológico de la zona estudiada (modificado a partir de Institut Cartogràfic i Geològic de Catalunya, 2006). Ver figura en color en la Web.

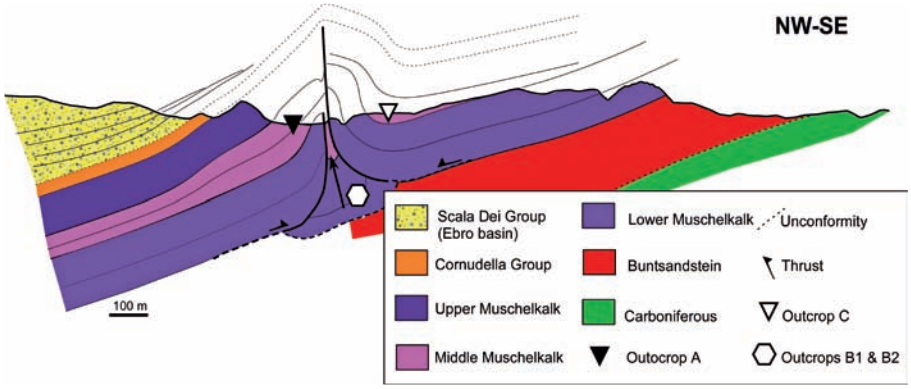

Fig. 2.- Cross-section of the study area. Location of the studied outcrops marked in the cross-section. Outcrops B1 and B2 correspond to the narrow synform band, while A and C correspond to the antiform fold limbs. See orientation of the cross-section in figure 1. See colour figure on the Web.

Fig. 2.- Corte geológico de la zona de estudio donde se indica las localizaciones de los afloramientos estudiados. Los afloramientos B1 y B2 corresponden a la banda de deformación del sinforme, mientras que A y C a los flancos del antiforme. Ver orientación de la sección en la figura 1. Ver figura en color en la Web.

and C outcrops) are less deformed and recrystallized. Prismatic recrystallization is much more abundant in veins located at the middle of the high strain zone (outcrops B1 and B2), where veins are interbedded in red siltstones, and not related with secondary gypsum hosts.

In the low deformed zones (outcrops A and C), veins display straight fibres oriented either normal or inclined (about ~30º) with regard to the walls. These veins usually appear at a low angle or parallel to bedding. There are also few veins showing sigmoidal or curved crystals, in which fibres are oriented at a high angle with respect to the vein walls and are subparallel to the walls in the centre. Veins of the NW flank of the anticlinorium (outcrop A) strike NE-SW and dip moderately to the NW, while fibres plunge approximately

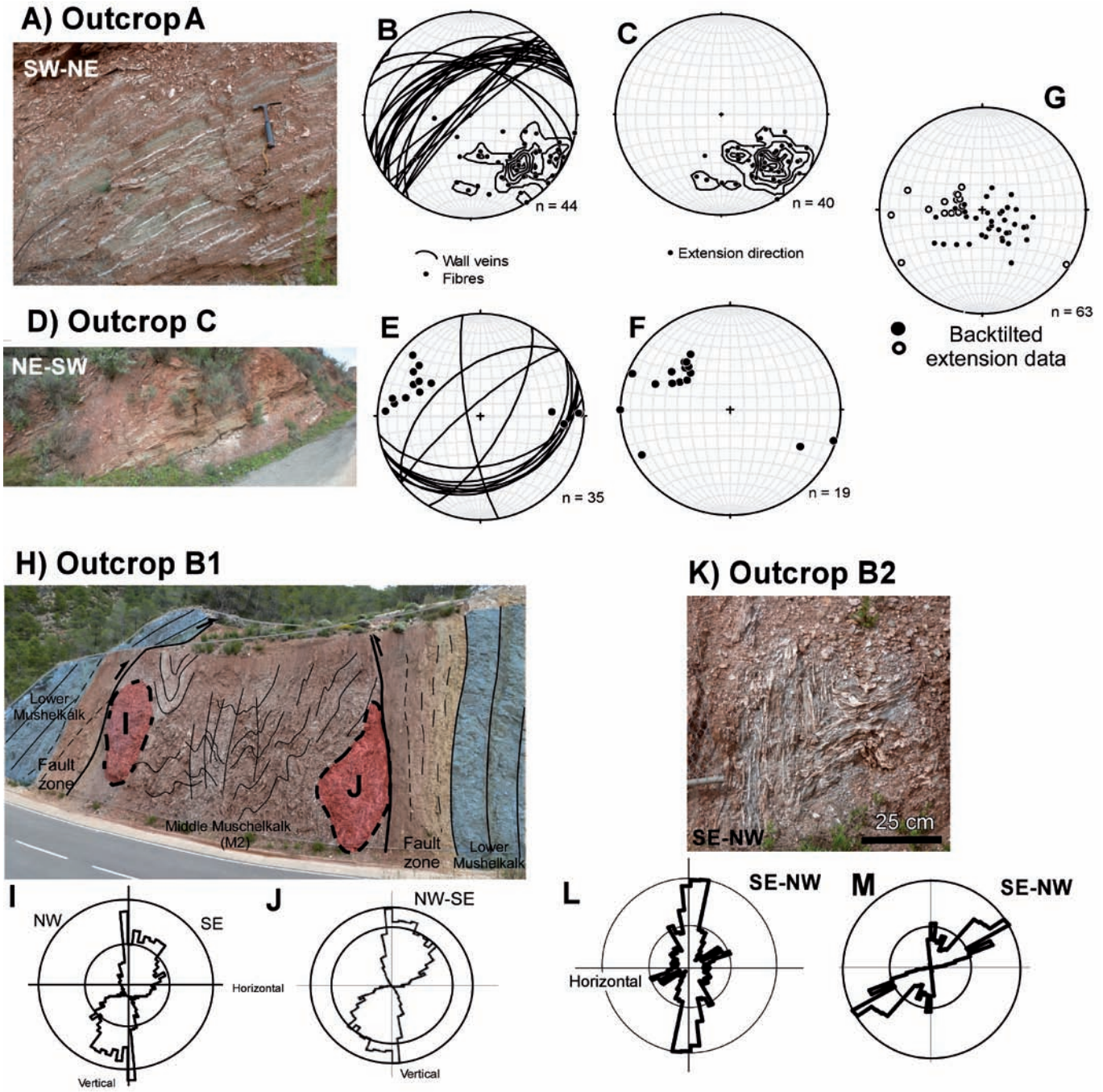

Fig. 3.- A)–C) Outcrop A: A) Field picture, B) Stereoplot of veins and fibres orientations and C) Stereoplot of the extensional directions. D)–F) Outcrop C: D) Field picture, E) Steroplot of veins and fibres orientations and F) Stereoplot of the extensional directions. G) Stereoplot of outcrops A and C after backtilting the data. H) Field picture of outcrop B1 with rose diagrams of gypsum veins strikes in zones (I) and (J). K) Field picture of outcrop B2 with rose diagrams of gypsum veins strikes (L), and calculated extensional directions (M) using the FraNEP code. See colour figure on the Web.

extensión calculadas. D)–F) Afloramiento C: D) Fotografía de campo, E) Proyección estereográfica de las venas y fibras y F) de las direcciones de extensión. G) Proyección estereografía de las direcciones de extensión desplegadas a la horizontal de los afloramientos A y C. H) Fotografía de campo interpretada del afloramiento B1, con los diagramas de rosa de los vientos mostrando las orientaciones de venas para los sectores (I) y (J). K) Fotografía de campo del afloramiento B2 con los diagramas de rosas de los vientos mostrando las orientaciones de las venas y las direcciones de extensión calculadas mediante del programa FraNEP. Ver figura en color en la Web.

140/36 on average (Fig. 3C). Veins of the SE flank (outcrop C, Fig. 3D) also strike NE-SW (Fig. 3E) but dip to the SE. The average fibres orientation of these veins is 300/28 (Fig. 3F). On both fold flanks fibres are oriented at a high angle with regard to the vein walls, thus suggesting that they formed from mode I or tensile fractures. The extension direction of the veins on the NW flank is 310/38 (Fig. 3C) and is 142/30 for veins on the SE flank (Fig. 3F).

Two main trends of vein orientations are recognizable in the high-strain domain (outcrops B1 and B2). The first set of veins forms at low angles with bedding, which is folded and has very similar strike to those of large-scale folds (*i.e.*, striking NW-SE and with east-dipping axial planes). The second set is composed of slightly folded veins with subvertical orientation, and crosscuts folded siltstones, gypsum layers and the first set of gypsum veins (at a low angle with bedding). The maximum frequency of the vein walls is found subvertical, and veins dominantly dip to the NW.

In addition to these two sets of veins, another important population of SE-dipping veins appears in outcrop B2 (Fig. 3L), but is missing in outcrop B1. These SE-dipping veins are folded in a similar way than the host rocks, but some of these veins are crosscutting other veins and folds. While we interpret the first two set of veins (NW dipping veins found in both outcrops) as pre- or syntectonic with the main deformation phase, the additional SE-dipping set found in outcrop B2 is clearly syntectonic. Fibre orientations at the outcrop B2 are very homogeneous, and plunge on average to the SE. Pre- and syntectonic fibres have a very similar orientation, although pretectonic veins tend to plunge less than syntectonic ones. Fibres of pretectonic veins are deformed and their orientation is very unlikely to indicate the extension direction. The calculated extension directions are very variable (Fig. 3M), but have three maxima frequency peaks. The maximum frequency is coincident with the fibre orientation and indicates the extensional direction during NW-SE folding. The other two peaks, at high and low dip angles, correspond to a pretectonic extensional direction, which is folded.

In order to test the chronology of the veins (before, during or after the fold) we have backtilted the data from low strain zones back considering initial horizontal layers (Fig. 3G). The results reveal that rotated data have a scattered distribution around the vertical axis, thus suggesting that at least a large number of veins formed before folding. Therefore, the formation of most of these veins is probably related to the rehydration of anhydrite layers during the Upper Cretaceous-Palaeogene exhumation (Juez-Larré and Andriessen, 2006), and before the main tectonic Alpine stage.

Finally, not all data in lower strain areas (outcrops A and C) are in agreement with this interpretation, as veins with sigmoidal or complex fibre patterns plot away from the vertical axis. Although we do not have enough data to interpret sigmoidal veins, a plausible hypothesis is that they are recording layer-parallel slip during folding and limb rotation during the Alpine orogeny.

Conclusions

A framework of gypsum veins cuts the host rock layers, composed of red siltstones and deformed gypsum rocks.

The relative chronology of the veins has been established according to the local Alpine structures (folds). The veins found at low angle to bedding predate folding and thus the main Alpine phase (*i.e.*, they are pre-folding). These veins are observed in all the outcrops. The formation of high-angle veins with respect to bedding and SE-dipping veins observed in outcrop B2 are interpreted here to have developed synchronous with the formation of the Montsant anticlinorium (*i.e.*, they are syn-folding).

Although gypsum veins are preferentially observed at the core of the structure, and therefore could be interpreted as indicators of fluid flow and overpressure related to compressive deformation, our structural analysis indicates that most of these veins are probably related to the exhumation and rehydration of anhydrite before the main tectonic Alpine stage. Such type of structural analysis has not been previously used in fibrous gypsum veins.

Acknowledgements

The present work was supported by the Grup Consolidat de Recerca Geologia Sedimentària 2009SGR-1451. We thank the editor Carlos L. Liesa and two anonymous reviewers for their helpful suggestions that contributed to improve this manuscript.

References

Couzens, B.A. and Wiltschko, D.V. (1996). *Bulletin of Canadian Petroleum Geology* 44, 165-179.

Durney, D.W. and Ramsay, J.G. (1973). In: *Gravity and Tectonics* (K.A. De Jong and J. Sholten, Eds.). Wiley, New York, 67-96.

El Tabakh, M., Schreiber, B.C. and Warren, J.K. (1998). *Journal of Sedimentary Research* 68, 88-89.

Guimerà, J. (1984). *Geological Magazine* 121, 413-420.

Institut Cartogràfic i Geologic de Catalunya (2006). Mapa Geológic Comarcal 1:50000, Full Priorat.

Juez-Larré, J. and Andriessen, P.A.M. (2006). *Earth and Planetary Science Letters* 243, 159-180.

Moragas, M., Martínez, C., Baqués, V., Playà, E., Travé, A., Alías, G. and Cantarero, I. (2013). *Geofluids* 13, 180-193.

Playà, E., Travé, A., Caja, M.A., Salas, R. and Martín-Martín, J.D. (2010). *Geofluids* 10, 314-333.

Teixell, A. (1988). *Revista de la Sociedad Geológica de España* 1, 229-238.

Zeeb, C., Gomez-Rivas, E., Bons, P.D., Virgo, S. and Blum, P. (2013). *Computers & Geosciences* 60,11-22.